SIMB Society for Industrial Microbiology and Biotechnology

Journal of Industrial Microbiology and Biotechnology, 2021, 48, kuab051

https://doi.org/10.1093/jimb/kuab051
Advance access publication date: 3 August 2021
Natural Products – Original Paper

Traminines A and B, produced by *Fusarium concentricum*, inhibit oxidative phosphorylation in *Saccharomyces cerevisiae* mitochondria

Katsuyuki Sakai [1], Yufu Unten[2], Aoi Kimishima[1,3], Kenichi Nonaka[1,3], Takumi Chinen[4], Kazunari Sakai[1,3], Takeo Usui [4], Kazuro Shiomi [1,3], Masato Iwatsuki [1,3], Masatoshi Murai [2], Hideto Miyoshi [2], Yukihiro Asami [1,3], Satoshi Ōmura[3]

[1]Graduate School of Infection Control Sciences, Kitasato University, 5-9-1 Shirokane, Minato-ku, Tokyo 108–8641, Japan
[2]Division of Applied Life Sciences, Graduate School of Agriculture, Kyoto University, Kitashirakawa Oiwake-cho, Sakyo-ku, Kyoto 606–8502, Japan
[3]Ōmura Satoshi Memorial Institute, Kitasato University, 5-9-1, Shirokane Minato-ku, Tokyo 108–8641, Japan
[4]Graduate School of Life and Environmental Sciences, University of Tsukuba, 1-1-1 Tennodai, Tsukuba, Ibaraki 305–8572, Japan
Correspondence should be addressed to: Yukihiro Asami. E-mail: yasami@lisci.kitasato-u.ac.jp

Abstract: Two new tetramic acid derivatives, traminines A (**1**) and B (**2**), were isolated from a culture broth of *Fusarium concentricum* FKI-7550 by bioassay-guided fractionation using multidrug-sensitive *Saccharomyces cerevisiae* 12geneΔ0HSR-iERG6. The chemical structures of **1** and **2** were elucidated by NMR studies. Compounds **1** and **2** inhibited the growth of the multidrug-sensitive yeast strain on nonfermentable medium containing glycerol, but not on fermentable medium containing glucose. These results strongly suggest that they target mitochondrial machineries presiding over ATP production via oxidative phosphorylation. Throughout the assay monitoring overall ADP-uptake/ATP-release in yeast mitochondria, **1** and **2** were shown to inhibit one or more enzymes involving oxidative phosphorylation. Based on biochemical characterization, we found that the interference with oxidative phosphorylation by **1** is attributable to the dual inhibition of complex III and F_oF_1-ATPase, whereas that by **2** is solely due to the inhibition of complex III.

Keywords: *Saccharomyces cerevisiae*, Multidrug-sensitive, Mitochondria

Introduction

Microorganisms produce secondary metabolites that have tremendous diversity in chemical structures, biological activities, and target proteins. These natural products potentially have numerous applications in the research and development of pharmaceuticals and agrochemicals. Leucomycin, staurosporine, and avermectin are well-known examples of such products, which have been exploited as drugs in clinical practice (Newman & Cragg, 2020; Ōmura et al., 2018).

The mitochondrial machineries presiding over ATP synthesis via oxidative phosphorylation are promising targets of biologically active compounds derived from microbial metabolites. A variety of naturally occurring chemicals have been reported to inhibit mitochondrial respiratory enzymes and F_oF_1-ATPase, some of which are being investigated as excellent drug candidates (Bald et al., 2017; Kita et al., 2007; Weinberg & Chandel, 2015). In this study, we conducted a comprehensive screening for natural products targeting the mitochondrial machineries using a yeast-screening system.

This screening system uses the budding yeast *Saccharomyces cerevisiae*, which is useful for identifying and evaluating biologically active compounds. However, the high drug resistance of the yeast is often an obstacle in discovering new compounds. One factor in the mechanism of drug resistance in *S. cerevisiae* is the ATP-binding cassette (ABC) transporter family, which effluxes exogenously added compounds from the cells. Therefore, the use of *S. cerevisiae* lacking the genes of ABC transporters was expected to be useful for the discovery of biologically active compounds that could not be identified by existing methods. In this work, the *S. cerevisiae* 12geneΔ0HSR-iERG6 strain (Chinen et al., 2014), a multidrug-sensitive strain in which 12 genes related to ABC transporters have been disrupted, was introduced into the screening system. We selected microbial culture broths, in which the growth of the *S. cerevisiae* 12geneΔ0HSR-iERG6 was inhibited in glycerol-containing medium (YPG agar medium; 1% yeast extract, 2% peptone, 3% glycerol, and 1.5% agar) but not in glucose-containing medium (YPD agar medium; 1% yeast extract, 2% peptone, 3% glucose, and 1.5% agar). This approach using two different carbon sources has been used to isolate compounds targeting mitochondrial oxidative phosphorylation (Sakai et al., 2019; Suga et al., 2015; Watanabe et al., 2017). Based on the above strategies, we revealed that *Fusarium concentricum* FKI-7550 produced two new tetramic acid derivatives; namely, traminines A (**1**) and B (**2**). Here, we report the fermentation, isolation, structural determination, and biological profiles of these new compounds.

Materials and Methods

General Experiments

Reverse- and normal-phase column chromatography was conducted on YMC-gel ODS-A (150 μm; YMC Co., Ltd., Kyoto, Japan) and Silica gel 60 (0.063–0.200 mm; Merck KGaA, Darmstadt, Germany), respectively. A Chromatorex C8 SPS100-5HE column was purchased from Fuji Silysia Chemical Co. (Aichi, Japan). High- and low-resolution mass data were measured on a JEOL JMS-T100LP (JEOL, Tokyo, Japan). NMR spectra were measured on a Bruker Avance III HD600 (Bruker Corp, Billerica, MA, USA) with

Received: April 9, 2021. **Accepted:** July 29, 2021.

^{1}H NMR at 600 MHz and ^{13}C NMR at 125 MHz in DMSO-d_6 and Varian XL-400 spectrometer (Agilent Technologies, Santa Clara, CA, USA) with ^{1}H NMR at 400 MHz and ^{13}C NMR at 100 MHz in DMSO-d_6. The chemical shifts were expressed in ppm and was referenced to DMSO-d_6 (2.48 ppm) in the ^{1}H NMR spectra and DMSO-d_6 (39.5 ppm) in the ^{13}C NMR spectra. IR spectra (ATR) were measured on an FT-210 Fourier transform IR spectrometer (Horiba Ltd., Kyoto, Japan). UV spectra were recorded on a Hitachi U-2801 spectrophotometer (Hitachi Ltd., Tokyo, Japan). Optical rotation was measured on a JASCO P-2200 polarimeter (JASCO Corporation, Tokyo, Japan).

Strain and Fermentation

Fungal strain FKI-7550 was isolated from soil around the root of *Cerasus* × *yedoensis* collected in Tokushima, Japan. We have already reported that the fusaramin producing strain FKI-7550 was assigned to the genus and was designated as *Fusarium concentricum* (NITE-2944 [Sakai et al., 2019]). One loopful of strain *Fusarium concentricum* FKI-7550 grown on an LcA slant (0.1% glycerol, 0.08% KH_2PO_4, 0.02% K_2HPO_4, 0.02% $MgSO_4{\cdot}7H_2O$, 0.02% KCl, 0.2% $NaNO_3$, and 1.5% agar, pH 6.0) was inoculated into a 500 ml-Erlenmeyer flask containing 100 ml of a pre-seed culture medium [2% glucose, 0.2% yeast extract, 0.05% $MgSO_4{\cdot}7H_2O$, 0.5% Polypeptone (FUJIFILM Wako Pure Chemical Co., Osaka, Japan), 0.1% KH_2PO_4, and 0.1% agar, pH 6.0] and incubated on a rotary shaker at 27°C for 4 days. Fifty-hundred ml of seed culture was prepared by the pre-seed culture medium. Twenty-five ml of the seed culture was inoculated into each of 200 Ulpack 47 culture bags (Hokken Co., Ltd., Tochigi, Japan) containing a production medium (500 g of water-sodden rice). Static fermentation was continued at 27°C for 12 days.

Evaluation of MIC Values of 1 and 2

We evaluated the minimum inhibitory concentration (MIC) of each compound against yeasts using a broth microdilution method (Sakai et al., 2019). The test compounds were dissolved in MeOH. The yeasts (1.0×10^4 cells/100 μL/well in a 96-well plate) were cultured in either YPD or YPG liquid medium with 0.00001% TWEEN 20 (Sigma-Aldrich, Co., St. Louis, MO, USA) in the presence of various concentrations of **1** and **2** for 2 and 3 days, respectively. Minimum inhibitory concentration values were evaluated by measuring OD_{600} on a Corona Grating Microplate Reader SH-9000 (Corona Electric, Ibaraki, Japan).

Yeast Culture and Isolation of Mitochondria

S. cerevisiae W303-1B (MATα *ade2-1 leu2-3,112 his3-22,15 trp1-1 ura3-1 can1-100*) cells were grown in semisynthetic lactate medium, and mitochondria were isolated by digesting the cell wall with Zymolyase-20T followed by homogenization and differential centrifugation, as described previously (Glick & Pon, 1995; Unten et al., 2019). The final mitochondrial pellet was resuspended in buffer containing 0.60 M mannitol, 10 mM Tris/HCl (pH 7.4), 0.1 mM EDTA, 0.1% BSA, and protease inhibitor cocktail (Sigma-Aldrich). Protein concentrations were determined using the BCA Protein Assay Kit (Thermo Fisher Scientic, Maltham, MA, USA) with BSA as the standard.

Measurement of ADP-Uptake/ATP-Release in Yeast Mitochondria

The measurement of ADP-uptake/ATP-release in isolated yeast mitochondria was conducted according to the procedures as described previously (Unten et al., 2019). Freshly prepared mitochondria (50 μg of proteins/ml) were suspended in 2.5 ml of reaction buffer (0.60 M mannitol, 0.10 mM EGTA, 2.0 mM $MgCl_2$, 10 mM KP_i, 5.0 mM α-ketoglutarate, and 10 mM Tris-HCl, pH 7.4) at 30°C in the presence of an ATP-detecting system (2.5 mM glucose, hexokinase [1.7 Enzyme Units (EU)], glucose-6-phosphate dehydrogenase (0.85 EU), 0.20 mM $NADP^+$, and 10 μM Ap_5A [a specific inhibitor of mitochondrial adenylate kinase]). Externally added ADP (100 μM) started the exchange reaction with ATP synthesized in the mitochondrial matrix. The formation of NADPH, which is proportional to ATP efflux, was monitored spectrophotometrically for 10 min at 340 nm ($\varepsilon = 6.2$ mM^{-1} cm^{-1}) with a Shimadzu UV-3000 (Shimadzu Co., Kyoto, Japan).

Measurement of Respiratory Enzyme and F_oF_1-ATPase Activities in Yeast Mitochondria

For the assays of each respiratory complex, yeast mitochondria were permeabilized by repeated freeze thawing in 50 mM KPi buffer (pH 7.4) to improve the accessibility of substrates, such as NADH, ATP, and cytochrome *c* (cyt. *c*) (Kelso et al., 2001; Unten et al., 2019). NADH-Q_1 oxidoreductase activity (NDH-2) was followed by the oxidation of NADH (340 nm; $\varepsilon = 6.2$ mM^{-1} cm^{-1}) in buffer (2.5 ml) containing 50 mM KPi (pH 7.4), 0.4 μM antimycin A 4.0 mM KCN, and 100 μM ubiquinone-1 (Q_1) at 30°C. The protein concentration was set to 12 μg/ml, and the reaction was initiated by the addition of NADH (final 50 μM).

Succinate-cyt. *c* oxidoreductase activity (complexes II–III) was followed by the reduction of cyt. *c* (550–540 nm; $\varepsilon = 21$ mM^{-1} cm^{-1}) in buffer (2.5 ml) containing 50 mM KPi (pH 7.4), 4.0 mM KCN, and 50 μM cyt. *c* (from horse heart, Sigma-Aldrich) at 30°C. The protein concentration was set to 12 μg/ml, and the reaction was initiated by the addition of sodium succinate (final 5.0 mM). NADH-cyt. *c* oxidoreductase activity (NDH-2-complex III) was followed by the same conditions using 50 μM NADH as an electron donor.

Cytochrome *c* oxidase activity (complex IV) was followed by the oxidation of reduced cyt. *c* (550–540 nm; $\varepsilon = 21$ mM^{-1} cm^{-1}) in 50 mM KPi buffer containing 0.5 μM antimycin A (pH 7.4, 2.5 ml) at 30°C. The protein concentration was set to 12 μg/ml, and the reaction was initiated by the addition of dithionite-reduced cyt. *c* (final 30 μM).

Hydrolysis of ATP FoF1-ATPase [complex V] was measured in 2.5 ml of reaction buffer containing 50 mM Tris/HCl (pH 8.0), 0.50 μM antimycin A, and 6.0 mM $MgCl_2$ at 30°C in the presence of ATP-generating system (2.0 mM 2-phosphoenolpyruvate, 50 μl of a pyruvate kinase/lactate dehydrogenase mixture [Sigma-Aldrich], and 100 μM NADH). The protein concentration was set to 12 μg/ml, and the reaction was initiated by the addition of ATP (final 4.0 mM). The oxidation of NADH, which is proportional to ATP hydrolysis, was monitored spectrophotometrically at 340 nm ($\varepsilon = 6.2$ mM^{-1} cm^{-1}).

Measurement of Complex III Activity in Bovine Heart Submitochondrial Particles

Bovine submitochondrial particles (SMPs) were prepared by the method of Matsuno-Yagi and Hatefi (Matsuno-Yagi & Hatefi, 1985), and complex III activity was followed by the reduction of cyt. *c* with a Shimadzu UV-3000 (550–540 nm, $\varepsilon = 21$ mM^{-1}cm^{-1}) using *n*-decylubiquinol (DBH_2) as an electron donor (Yabunaka et al., 2002). To improve the accessibility of cyt. *c*, SMPs (7.5 mg/ml) were treated with sodium deoxycholate (0.9% (wt/vol), 1 h, on ice) before dilution with reaction medium. Then, the SMPs (10 μg of proteins/ml) were incubated with an inhibitor for 4 min in a reaction medium (2.5 ml) containing 0.25 M sucrose, 1.0 mM $MgCl_2$, 4 mM KCN, 60 μM cyt. *c* (from horse heart), and 50 mM KPi (pH 7.4). The reaction was initiated by the addition of 50 μM DBH_2.

Table 1 NMR Spectroscopic Data for Traminine A (**1**) in DMSO-d_6

Position	δ_C	*mult.*	δ_H *(int., mult., J in Hz)*	*HMBC*
1	191.2	C		
2	36.2	CH	3.50 (1H, qt, J = 6.8, 7.3)	C-1, C-3, C-4, C-17
3	36.1	CH_2	2.17 (1H, ddd, J = 14.2, 7.3, 7.2)	C-1, C-2, C-4, C-5, C-17
			2.33 (1H, ddd, J = 14.2, 7.3, 7.2)	
4	123.9	CH	5.41 (1H, dt, J = 15.6, 7.2)	C-2, C-3, C-6
5	136.6	CH	5.99 (1H, d, J = 15.6)	C-3, C-6, C-7, C-18
6	131.3	C		
7	137.2	CH	5.14 (1H, d, J = 9.2)	C-5, C-8, C-9, C-18, C-19
8	30.4	CH	2.63 (1H, m)	C-6, C-7, C-9, C-10, C-19
9	47.2	CH_2	1.93 (2H, m)	C-7, C-10, C-11, C-20
10	134.1	C		
11	126.1	CH	5.71 (1H, d, J = 10.8)	C-9, C-12, C-13, C-20
12	126.8	CH	6.17 (1H, dd, J = 15.2, 10.8)	C-10, C-11, C-14
13	131.9	CH	5.50 (1H, dt, J = 15.2, 7.3)	C-11, C-14, C-15
14	34.3	CH_2	2.01 (2H, dt, J = 7.3, 7.1,)	C-12, C-13, C-15, C-16
15	22.2	CH_2	1.34 (2H, qt, J = 7.5, 7.1)	C-14, C-16
16	13.6	CH_3	0.84 (3H, t, J = 7.5)	C-14, C-15
17	16.0	CH_3	1.04 (3H, d, J = 6.8)	C-1, C-2
18	12.4	CH_3	1.62 (3H, brs)	C-5, C-6, C-7
19	20.4	CH_3	0.84 (3H, d, J = 6.8)	C-7, C-8, C-9
20	16.3	CH_3	1.63 (3H, s)	C-9, C-10, C-11
2′	177.9	C		
3′	103.1	C		
4′	193.5	C		
5′	65.8	CH	3.79 (1H, d, J = 2.1)	C-2′, C-4′, C-6′, C-7′
6′	66.2	CH	4.20 (1H, ddd, J = 8.8, 4.6, 2.1)	C-7′, C-8′
7′	39.0	CH_2	2.52 (1H, dd, J = 15.5, 8.8)	C-6′, C-8′
			2.63 (1H, dd, J = 15.5, 4.6)	
8′	171.1	C		
9′	51.3	CH_3	3.58 (s)	C-8′

Note. Data were collected at 400 MHz for ^{1}H and 100 MHz for ^{13}C.

The redox statuses of cytochromes *b* (containing hemes b_L and b_H) and c_1 (containing heme c_1) were monitored spectrophotometrically at 563–575 and 539–553 nm, respectively (Link et al., 1993; Matsuno-Yagi & Hatefi, 1996). The absorbance change was recorded with a Shimadzu UV-3000 spectrophotometer in a dual wavelength mode. Bovine SMPs (1.2 mg/ml) were suspended in 2.0 ml reaction buffer (250 mM sucrose, 50 mM KPi, 1.0 mM $MgCl_2$, 4.0 mM KCN, and 0.2 μM SF6847, pH 7.4) at 30°C and the reaction was initiated by the addition of 5 mM sodium succinate after the equilibration of SMPs with an inhibitor(s) for 4 min. The concentration of each inhibitor was set to that exhibiting maximum inhibition of complex III activity. Complete reduction of the hemes was achieved by the addition of excess sodium dithionite in the cuvette.

Results and Discussion

Extraction and Isolation of 1 and 2

The stationary culture (100 kg) was extracted with acetone (120 l) and the extract was filtrated. The filtrate was concentrated *in vacuo* to remove acetone. The remaining aqueous solution (35 l) was extracted two times with an equal volume of EtOAc (total 70 l). The organic layer was concentrated to dryness to afford a crude extract (628 g). The extract was chromatographed on a Diaion HP20 column and eluted stepwise with a mixture of MeOH-H_2O (20:80, 50:50, and 100:0, each 3 l). Compounds were eluted with the 100:0 eluate, and the solution was concentrated *in vacuo* to remove MeOH. The 100:0 fraction (129 g) was applied to an ODS gel column (55 i.d. × 215 mm) and eluted stepwise with a mixture of MeOH-H_2O (20:80, 50:50, 70:30, 80:20, 90:10, and 100:0; each 2 l). The 80:20 fraction was concentrated to dryness to afford a crude extract (33 g). The extract was chromatographed on a silica gel column and eluted stepwise with a mixture of $CHCl_3$-MeOH (100:0, 100:1, 100:5, 90:10, 1:1, and 0:100, each 2 l). The active fraction (90:10) was concentrated *in vacuo* to remove organic solvent. Finally, the concentrated material (1.6 g) was applied to an HPLC (Chromatorex C8 SPS100-5HE, 20 i.d. × 250 mm) with an isocratic solvent system of 70% acetonitrile-water with 0.1% trifluoroacetic acid solution at a flow rate of 10 ml/min to give two new compounds, traminines A (11.5 mg; retention time 64–82 min; **1**) and B (70.7 mg; retention time 48–52 min; **2**) in Figs. 1a and b.

Traminine A (**1**): yellow oil; soluble in DMSO, MeOH, acetone and $CHCl_3$; insoluble in H_2O; $[\alpha]_D^{27}$ −140 (c = 0.1, MeOH); IR ν_{max} (ATR) cm^{-1} 3324, 2958, 2927, 1721, 1655, 1608, 1440, 1375, 1208, 1084, and 963; UV (MeOH) λ_{max} nm (ε) 243 (52790) and 281 (15630).

Traminine B (**2**): yellow oil; soluble in DMSO, MeOH, acetone and $CHCl_3$; insoluble in H_2O; $[\alpha]_D^{27}$ −15 (c = 0.1, MeOH); IR ν_{max} (ATR) cm^{-1} 3394, 2958, 2925, 2870, 1770, 1715, 1601, 1438, 1318, 1238, 1074, 1040, and 963; UV (MeOH) λ_{max} nm (ε) 243 (49320) and 275 (14970).

Structure Elucidation of 1 and 2

The molecular formula of **1** was elucidated as $C_{28}H_{41}NO_6$ by HR-ESI-MS data ([M–H]$^-$, m/z 486.2856: calculated for $C_{28}H_{40}NO_6$, 486.2857), requiring nine degrees of unsaturation. All connections for ^{1}H and ^{13}C in **1** were elucidated by HSQC study (Table 1). The NMR data measured in DMSO-d_6 and the molecular

Table 2 NMR Spectroscopic Data for Traminine B (**2**) in DMSO-d_6

Position	δ_C	*mult.*	δ_H *(int., mult., J in Hz)*	*HMBC*
1	197.0	C		
2	39.5	CH	3.51 (1H, qt, J = 7.2, 7.8)	C-1, C-3, C-4, C-17
3	35.7	CH_2	2.01 (1H, ddd, J = 15.0, 7.8, 7.2)	C-1, C-2, C-4, C-5, C-17
			2.36 (1H, ddd, J = 15.0, 7.8, 7.2)	
4	124.7	CH	5.43 (1H, dt, J = 15.6, 7.2)	C-2, C-3, C-6
5	136.3	CH	5.98 (1H, d, J = 15.6)	C-3, C-6, C-7, C-18
6	131.4	C		
7	136.9	CH	5.13 (1H, d, J = 9.0)	C-5, C-8, C-9, C-18, C-19
8	30.4	CH	2.63 (1H, m)	C-6, C-7, C-9, C-10, C-19
9	47.2	CH_2	1.94 (2H, m)	C-7, C-8, C-10, C-11, C-19, C-20
10	134.1	C		
11	126.1	CH	5.71 (1H, d, J = 10.8)	C-9, C-12, C-13, C-20
12	126.9	CH	6.17 (1H, dd, J = 15.2, 10.8)	C-10, C-11, C-14
13	132.0	CH	5.51 (1H, dt, J = 15.2, 7.3)	C-11, C-14, C-15
14	34.4	CH_2	2.00 (2H, td, J = 7.5, 7.3)	C-12, C-13, C-15
15	22.2	CH_2	1.33 (2H, qt, J = 7.2, 7.5)	C-13, C-14, C-16
16	13.6	CH_3	0.83 (3H, t, J = 7.2)	C-14, C-15
17	16.1	CH_3	0.97 (3H, d, J = 7.2)	C-1, C-2, C-3
18	12.4	CH_3	1.63 (3H, s)[a]	C-5, C-6, C-7
19	20.4	CH_3	0.84 (3H, d, J = 7.2)	C-8, C-9
20	16.3	CH_3	1.63 (3H, s)[a]	C-9, C-10, C-11
2′	167.0	C		
3′	105.1	C		
4′	188.6	C		
5′	67.7	CH	4.60 (1H, d, J = 3.3)	C-2′, C-3′, C-4′
6′	67.0	CH	4.51 (1H, dd, J = 3.3, 3.6)	C-5′, C-7′, C-8′
7′	46.0	CH_2	2.27 (1H, d, J = 16.8)	C-4′, C-5′, C-6′, C-8′
			2.95 (1H, dd, J = 16.8, 3.6)	
8′	172.0	C		

Note. [a]Overlapped.
Data were collected at 600 MHz for ^{1}H and 150 MHz for ^{13}C.

formula indicated the presence of six methyls, four sp^3 methines including one nitrogenated and one oxygenated, six sp^2 methines, five sp^3 methylenes including one carboxylated, and seven fully-substituted sp^2 quaternary including one hydroxylated and three carbonyls carbons (Table 1). The ^{1}H NMR spectrum of **1** indicated the presence of six methyls, four sp^3 methines, five sp^3 methylenes, and six sp^2 methine. ^{1}H-^{1}H COSY of **1** indicated alignments from H-2 (δ_H 3.50) to H-5 (δ_H 5.99); from H-7 (δ_H 5.14) to H_2-9 (δ_H 1.93); and H-11 (δ_H 5.71) to H_3-16 (δ_H 0.84), plus connections between H-2 and H_3-17 (δ_H 1.04), H-8 (δ_H 2.63), and H_3-19 (δ_H 0.84) as shown in Fig. 2a. The HMBC correlations from H-2, H_2-3 (δ_H 2.17 and 2.33), and H_3-17 to C-1 (δ_C 191.2); from H-5 to C-6 (δ_C 131.3), C-7 (δ_C 137.2), and C-18 (δ_C 12.4); from H-7 to C-5 (δ_C 136.6) and C-18; from H_3-18 (δ_H 1.62) to C-5, C-6, and C-7; from H_2-9 to C-10 (δ_C 134.1), C-11 (δ_C 126.1), and C-20 (δ_C 16.3); from H-11 to C-9 (δ_C 47.2), C-13 (δ_C 131.9), and C-20; and from H_3-20 (δ_H 1.63) to C-9, C-10, and C-11 suggested the presence of a hydrocarbon moiety. Moreover, eight remaining ^{13}C signals of **1** at δ_C 177.9 (C-2′), 103.1 (C-3′), 193.5 (C-4′), 65.8 (C-5′), 66.2 (C-6′), 39.0 (C-7′), 171.1 (C-8′), and 51.3 (C-9′) were assigned as β-hydroxyglutamic acid conjugated tetramic acid moiety after comparing with other tetramic acids (Fig. 2a) (Fukuda et al., 2015; Kemami-Wangun & Hertweck, 2007; Sakai et al., 2019; Shang et al., 2015; Xu et al., 2010). Due to the tautomerism of tetramic acid, the ^{13}C signals of C-1, C-2′, C-3′, C-4′, and C-5′ were suggested to be broad. It was supported by five remaining degrees of unsaturation. Finally, the planar structure of **1** was elucidated by the HMBC correlations from methoxy protons (δ_H 3.58) and H_2-7′ (δ_H 2.52 and 2.63) to C-8′; from H-6′ (δ_H 4.20) to C-7′; and from H-5′ to C-2′, C-4′, C-6′, and C-7′ deduced the connection between C-5′ and the β-hydroxyglutamic acid group. The geometry of double bonds at C-4 and C-5, and C-12 and C-13 were determined to be of the (*E*)-configuration on the basis of the large vicinal coupling constants ($J_{4\text{-}5}$ = 15.6 and $J_{12\text{–}13}$ = 15.2 Hz, respectively). Furthermore, the geometry of double bonds at C-6 and C-7, and C-10 and C-11 were also determined to be of the (*E*)-configuration on the basis of the significant ROESY between H-5 and H-7 as well between H-9 and H-11, respectively (Supplementary Fig. S6). Therefore, based on the spectral data, the structure of **1** was elucidated as a new compound containing the tetramic acid moiety and named traminine A (**1**).

The similarity in both physicochemical properties and NMR spectrum between **1** and **2** strongly suggested that **2** is a new analog of **1**. The molecular formula of **2** was elucidated as $C_{27}H_{37}NO_5$ by HR-ESI-MS data ($[M + H]^+$, m/z 456.2728: calculated for $C_{27}H_{38}NO_5$, 456.2750), requiring ten degrees of unsaturation. The ^{1}H and ^{13}C NMR spectra data of **2** is listed in Table 2. NMR spectra of **2** lacked a methoxy group and changed the carbon chemical shifts at C-2′ (δ_C 167.0), C-4′ (δ_C 188.6), and C-7′ (δ_C 46.0), the tetramic acid moiety of **1**. The HMBC experiments (Fig. 2b) and six remaining degrees of unsaturation gave the following results; the proposed fused ring core structure containing tetramic acid moiety was confirmed by the key HMBC correlations: from H-5′ (δ_H 4.60) to C-2′, C-3′ (δ_C 105.1), and C-4′; from H-6′ (δ_H 4.51) to C-7′ and C-8′ (δ_C 172.0); from H_2-7′ (δ_H 2.27 and 2.95) to C-5′ (δ_C 67.7), C-6′ (δ_C 67.0), and C-8′; and from H_2-7′ to N-1′ (δ_N −221.7, Supplementary Fig. S12) position by ^{1}H-^{15} N HMBC correlation. ^{1}H-^{1}H COSY of **2** indicated alignments from H-5′ to H_2-7′ as shown in Fig. 2b. The chemical shifts of the side chain, both the ^{1}H-^{1}H COSY and HMBC

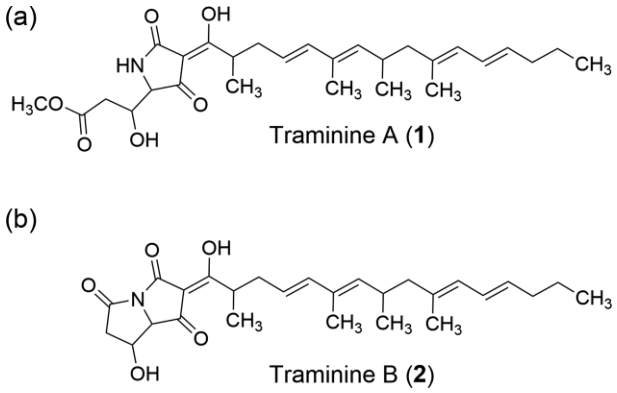

Fig. 1 Chemical structures of traminines A (**1**) and B (**2**).

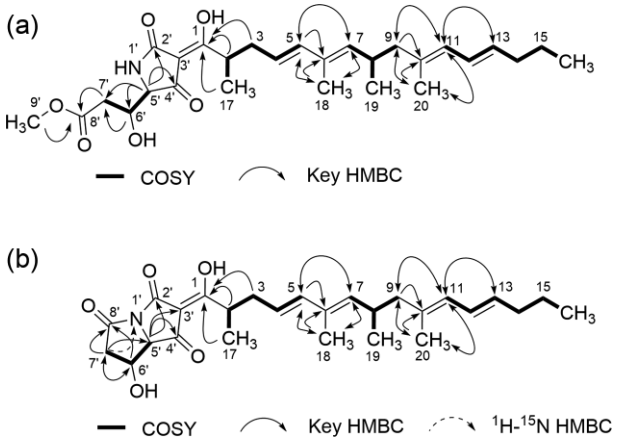

Fig. 2 Structure elucidation of traminines A (**1**) and B (**2**). ^{1}H-^{1}H COSY (bold lines), key HMBC (arrows), and key ^{1}H-^{15}N HMBC correlation (dash arrow).

correlations (from C-1 to C-20) is almost the same as those of **1**. The geometry of double bonds at C-4 and C-5; C-12 and C-13; C-6 and C-7; and C-10 and C-11 were also determined to be of the (*E*)-configuration on the basis of the large vicinal coupling constants (J_{4-5} = 15.6 and J_{12-13} = 15.2 Hz, respectively) and ROESY experiment (Supplementary Fig. S13). Therefore, the planar structure of **2** was elucidated as shown in Fig. 1b and we designated **2** to be traminine B.

Compound **1** was a novel compound that, unlike harzianic acid and JBIR-22, contained a β-hydroxyglutamic acid group bound to tetramic acid (Izumikawa et al., 2010; Kawada et al., 2004). Also, it contained a polyketide side chain with a distinctive structure. Interestingly, this polyketide structure has never been found previously in natural products. Compound **2** had a structure similar to that of **1**, but with a distinctive novel cyclic tetramic acid structure. Although **2** was a little similar to talarotoxin and burnettramic acids (Ishii et al., 1995; Li et al., 2019), its structure is very rare among natural products. The structure of the polyketide side chain in **2** was also distinctive. When evaluating the biological activity, care was taken about the stability of **2**. The purity of **2** used for the evaluation of biological activity was tested in the Supplementary Fig. S14.

Evaluation of MIC Values of 1 and 2 Against Yeasts

We measured the MICs of **1** and **2** against wild type and multidrug-sensitive *S. cerevisiae* (Table 3). Compounds **1** and **2** did not demonstrate strong inhibition against the wild type yeast BY4741 grown on YPD medium. It is interesting that **1** and **2** showed strong inhibition against the multidrug-sensitive yeast grown on YPG medium. The selectivity of **1** and **2** was > 64 and > 128 times, respectively. Compounds **1** and **2** did not show growth inhibition against the wild type yeast, it is strongly suggested that the multidrug-sensitive budding yeast is a useful tool to find new growth inhibition compounds. Therefore, we assumed that the target of **1** and **2** is any one of the mitochondrial functions, such as the electron transfer system. Evaluation of the growth inhibition of the yeast by **1** and **2** suggested that they may be inhibitors of mitochondrial functions because these compounds inhibited the growth of the multidrug-sensitive budding yeast *S. cerevisiae* 12geneΔ0HSR-iERG6 grown on YPG agar medium but did not on YPD agar medium.

Table 3 MIC Values of **1** and **2** Against Yeast

Compound	MIC values (μg/ml)			
	BY4741		12geneΔ0HSR-iERG6	
	YPD	YPG	YPD	YPG
1	>128	>128	>128	2
2	>128	32	>128	1

Table 4 The IC_{50} Values of the Test Compounds in Overall ADP-Uptake/ATP-Release Reactions with Isolated *S. cerevisiae* Mitochondria

Compound	IC_{50} (nmol/mg of proteins)
traminine A (**1**)	120 ± 10
traminine B (**2**)	3.8 ± 0.6
CATR	0.13 ± 0.01
antimycin A	0.10 ± 0.01

Note. The IC_{50} value is the concentration (nmol/mg of proteins) needed to reduce the control ATP efflux from yeast mitochondria by 50%. The average ATP efflux in the absence of inhibitor was 0.16 ± 0.01 μmol ATP/min/mg of proteins. Values are means ± standard error.

Effects of 1 and 2 on the ATP Synthesis in Yeast Mitochondria

Since yeast glycerol metabolism depends on oxidative phosphorylation, the increased sensitivity to **1** and **2** in glycerol medium strongly suggests that they target mitochondrial machineries presiding over ATP production via oxidative phosphorylation. Based on the assay monitoring overall ADP-uptake/ATP-release in yeast mitochondria energized by α-ketoglutarate (Unten et al., 2019), we evaluated the effects of **1** and **2** on ATP synthesis via oxidative phosphorylation. This assay system generally enables us to determine potential inhibitors for any of the mitochondrial proteins presiding over ATP synthesis via oxidative phosphorylation, such as respiratory enzymes (type-2 NADH dehydrogenase [NDH-2], and complexes II-IV), F_oF_1-ATPase (complex V), and mitochondrial transporters (VDAC, ADP/ATP carrier, and phosphate carrier). As listed in Table 4, **1** and **2** inhibited overall ADP-uptake/ATP-release reactions with IC_{50} values of 120 and 3.8 nmol/mg of proteins, respectively. We confirmed, as a control, that carboxyatractyloside (CATR, an inhibitor of ADP/ATP carrier) and antimycin A (an inhibitor of complex III) also inhibited the reaction (Table 4).

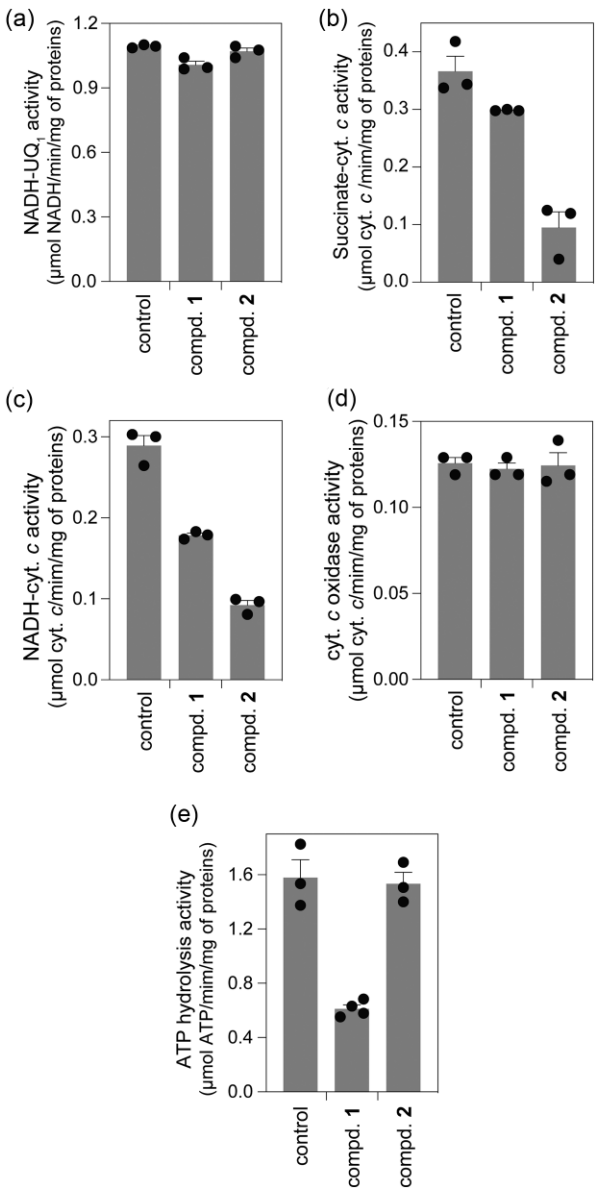

Fig. 3 Effects of traminines A (**1**) and B (**2**) on the respiratory enzyme activities. The effects of **1** and **2** on the activity of each respiratory complex. NADH-UQ_1 oxidoreductase (NDH-2, a), succinate-cyt. *c* oxidoreductase (complexes II–III, b), NADH-cyt. *c* oxidoreductase (NDH-2–complex III, c), and cyt. *c* oxidase (complex IV, d) activities in addition to ATP hydrolysis (FoF1-ATPase, e) were measured in the presence of **1** and **2**. In these assays, the concentration of **1** and **2** were set to 360 and 11 nmol/mg of proteins, respectively, which are equivalent to 3 × IC_{50} obtained in the ADP-uptake/ATP-release reactions. Values show means ± SEM (n = 3–4).

Identification of the Target Enzymes of 1 and 2

As the mitochondrial respiratory enzymes provide the major driving force for ADP uptake and ATP synthesis by generating electrochemical proton gradient, we examined the effects of **1** and **2** on each respiratory enzymes and F_oF_1-ATPase (Fig. 3). The concentrations of **1** and **2** were set to 360 and 11 nmol/mg of proteins, respectively, which are equivalent to 3 × IC_{50} obtained in the ADP-uptake/ATP-release reactions described above. As shown in Figs. 3a and 3d, both compounds exhibit no inhibition of NDH-2 and complex IV activities. Compound **2** inhibited succinate-cyt. *c* oxidoreductase (covering complexes II and III) and NADH-cyt. *c* oxidoreductase (covering NDH-2 and complex III) activities by approximately 70% (Fig. 3b and c). As both assays include electron flux through complex III, these results indicate that the potential target of **2** is respiratory complex III. On the other hand, **1** was found to inhibit ATP hydrolysis (Fig. 3e) as well as succinate- and NADH-cyt. *c* oxidoreductase activities (Fig. 3b and c). We note that, at higher concentration (40 × IC_{50}), **2** also inhibited ATP hydrolysis by around 30% (data not shown), but this effect was negligible at the concentration range equivalent to 1 ~ 5 × IC_{50} that was determined in the ADP-uptake/ATP-release assay. Altogether, inhibition of oxidative phosphorylation by **1** is attributed to the dual inhibition of complex III (ubiquinol-cyt. *c* oxidoreductase) and F_oF_1-ATPase with IC_{50} values of 1,100 and 200 nmol/mg of proteins, respectively; whereas that by **2** is due to the inhibition of complex III with IC_{50} value of 6.8 nmol/mg of proteins.

Identification of the Binding Site of 2 in Complex III

Complex III contains two reaction sites for ubiquinone/ubiquinol: one is proximal to the matrix side (Q_i site), where an electron is transferred from cytochrome *b* (containing hemes b_L and b_H) to ubiquinone, and the other is proximal to the intermembrane space (Q_o site), where an electron is transferred from ubiquinol to Rieske iron-sulfur cluster, followed by the reduction of cytochrome c_1 (containing heme c_1). Complex III inhibitors are generally classified into two groups called 'Q_i site' and 'Q_o site' inhibitors, which are represented by antimycin A and myxothiazol, respectively (Crofts, 2004; Trumpower, 1990). To identify the binding site of **2** in complex III (Q_i site or Q_o site), we examined the effects of **2** on the reduction kinetics of cytochromes *b* and *c* hemes using bovine heart SMPs. Prior to the analysis, we confirmed that **2** inhibits complex III in SMPs with IC_{50} value of 9.5 nmol/mg of proteins.

It is a well-known phenomenon that cytochrome *b* hemes are immediately reduced by the addition of respiratory substrate in the presence of Q_i or Q_o site inhibitor. In agreement of previous studies (Link et al., 1993; Matsuno-Yagi & Hatefi, 1996; Trumpower, 1990), only the simultaneous addition of Q_i and Q_o site inhibitors (antimycin A and myxothiazol, respectively) led to the suppression of the *b* hemes reduction (Fig. 4a, traces a–c and e). The addition of **2** alone did not affect the reduction level of the *b* hemes (trace d), while the simultaneous addition of **2** and antimycin A markedly inhibited the *b* hemes reduction (trace f). We noted that a slow increase in the *b* heme reduction was observed in the presence of antimycin A and myxothiazol, but not in the presence of antimycin A and **2** (traces e and f). A pair of myxothiazol and **2** did not suppress the *b* hemes reduction (trace g). Next, we investigated the effect of inhibitors on the c_1 heme reduction. Antimycin A did not affect the reduction level of the c_1 heme, whereas myxothiazol significantly reduced the reduction level (Fig. 4b, traces a–c) (Link et al., 1993; Matsuno-Yagi & Hatefi, 1996; Trumpower, 1990). The extent of suppression of the c_1 heme reduction by **2** was less than that by myxothiazol; however, once reduced, c_1 heme slowly reoxidized (trace d). Although we have no definite explanation of this phenomenon at present, this result suggests that structure of the c_1 heme environment could be destabilized by **2**. Taking all these results together, we conclude that **2** binds to the Q_o site in complex III, which is a slightly different manner from that of myxothiazol.

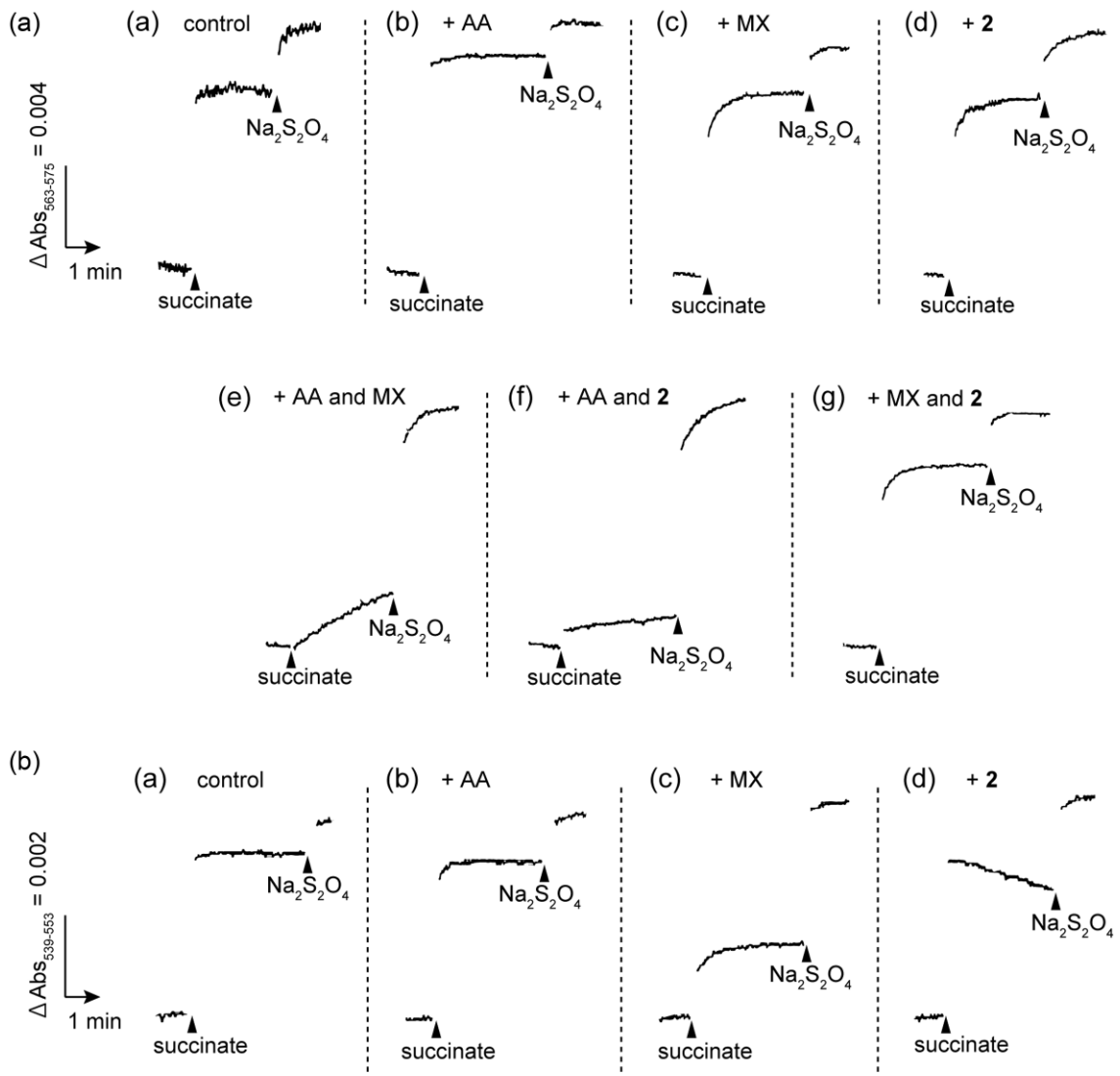

Fig. 4 Effects of traminine B (**2**) on the reduction of cytochrome *b* and *c* hemes of complex III in bovine SMPs. (a) The reduction of cytochrome *b* hemes was monitored at the wavelength pair of 563 and 575 nm. SMPs (1.2 mg/ml) were incubated with various inhibitors for 4 min before the addition of sodium succinate (5 mM). The complete reduction of the *b* hemes was achieved by the addition of $Na_2S_2O_4$. Traces are as follows: *a*, control; *b*, antimycin A (AA, 2 μM); *c*, myxothiazol (MX, 4 μM); *d*, traminine B (**2**, 23 μM); *e*, antimycin A and myxothiazol; *f*, antimycin A and **2**; *g*, myxothiazol and **2**. (b) The reduction of cytochrome c_1 heme was monitored at the wavelength pair of 539 and 553 nm. Traces are as follows: *a*, control; *b*, antimycin A; *c*, myxothiazol; *d*, **2**. Data are representative of three independent measurements. X axis is time, Y axis is ΔAbs.

Conclusion

Naturally occurring tetramic acids have attracted a great deal of attention for their broad spectrum of biological activities (Mo et al., 2014). Fusaramin (Sakai et al., 2019), equisetin (Köning et al., 1993), and equisetin-like compound TA-289 (Quek et al., 2013) have been reported to interfere with mitochondrial oxidative phosphorylation; however, to the best of our knowledge, there was no report on their target protein(s) in mitochondria. Throughout bioassay-guided screening with multidrug-sensitive *S. cerevisiae* 12geneΔ0HSR-iERG6 strain, we here isolated two new tetramic acid derivatives traminines A (**1**) and its intramolecular *N*-acylation product traminine B (**2**) from the culture broth of a fungal strain *Fusarimum concentricum* FKI-7550. Both compounds were found to inhibit ATP production via oxidative phosphorylation in *S. cerevisiae* mitochondria. Detailed biochemical characterization revealed that **1** elicits dual inhibition of respiratory complex III and F_oF_1-ATPase, whereas **2** inhibits solely complex III (at Q_o site). Further structural modifications of these compounds would contribute greatly to the development of new types of pharmaceutical and agrochemical lead compounds.

Acknowledgments

We thank Dr. K. Nagai and Ms. N. Sato (School of Pharmacy, Kitasato University) for various instrumental analyses. This article is dedicated to the fond memory of Professor Arnold L. Demain.

Supplementary Material

Supplementary material is available online at *JIMB* (*www.academic.oup.com/jimb*).

Author Contributions

Kazuro Shiomi, Hideto Miyoshi, Yukihiro Asami and Satoshi Ōmura designed the research. Katsuyuki Sakai, Aoi Kimishima

and Masato Iwatsuki isolated and analyzed the compounds. Yufu Unten, Masatoshi Murai and Hideto Miyoshi evaluated the biological activities. Kenichi Nonaka isolated and maintained the fungal strain. Takumi Chinen and Takeo Usui established the yeast strain. Katsuyuki Sakai, Kazunari Sakai, Yufu Unten, Masatoshi Murai, Hideto Miyoshi and Yukihiro Asami wrote the paper. All authors approved the final manuscript.

Funding

This study was partially supported by the Platform Project for Supporting Drug Discovery and Life Science Research (Basis for Supporting Innovative Drug Discovery and Life Science Research [BINDS]) from the Japan Agency for Medical Research and Development (AMED) under Grant Number JP20am0101096. Moreover, this research was partly supported by AMED under Grant Number 20ae0101047 as well. The study was supported by The Public Foundation of Elizabeth Arnold–Fuji, Japan.

Conflict of Interest

No potential conflict of interest was reported by the authors.

References

Bald, D., Villellas, C., Lu, P., & Koul, A. (2017). Targeting energy metabolism in *Mycobacterium tuberculosis*, a new paradigm in antimycobacterial drug discovery. *mBio*, 8(2), e00272–17.

Chinen, T., Nagumo, Y., & Usui, T. (2014). Construction of a genetic analysis-available multidrug sensitive yeast strain by disruption of the drug efflux system and conditional repression of the membrane barrier system. *The Journal of General and Applied Microbiology*, 60(4), 160–162.

Crofts, A. R. (2004). The cytochrome bc_1 complex: function in the context of structure. *Annual Review Physiology*, 66, 689–733.

Fukuda, T., Sudoh, Y., Tsuchiya, Y., Okuda, T., Matsuura, N., Motojima, A., Oikawa, T., & Igarashi, Y. (2015). Tolypoalbin, a new tetramic acid from *Tolypocladium album* TAMA 479. *The Journal of Antibiotics*, 68(6), 399–402.

Glick, B. S. & Pon, L. A. (1995). Isolation of highly purified mitochondria from *Saccharomyces cerevisiae*. *Methods in Enzymology*, 260, 213–223.

Izumikawa, M., Hashimoto, J., Hirokawa, T., Sugimoto, S., Kato, T., Takagi, M., & Shin-ya, K. (2010). JBIR-22, an inhibitor for protein-protein interaction of the homodimer of proteasome assembly factor 3. *Journal of Natural Products*, 73(4), 628–631.

Ishii, K., Itoh, T., Kobayashi, K., Horie, Y., & Ueno, Y. (1995). Isolation and characterization of a cytotoxic metabolite of *Talaromyces bacillosporus*. *Applied and Environmental Microbiology*, 61(3), 941–943.

Kemami-Wangun, H. V. & Hertweck, C. (2007). Epicoccarines A, B and epipyridone: tetramic acids and pyridone alkaloids from an *Epicoccum* sp. associated with the tree fungus *Pholiota squarrosa*. *Organic & Biomolecular Chemistry*, 5(11), 1702–1705.

Kita, K., Shiomi, K., & Ōmura, S. (2007). Advances in drug discovery and biochemical studies. *Trends in Parasitology*, 23(5), 223–229.

Kawada, M., Yoshimoto, Y., Kumagai, H., Someno, T., Momose, I., Kawamura, N., Isshiki, K., & Ikeda, D. (2004). PP2A inhibitors, harzianic acid and related compounds produced by fungus strain F-1531. *The Journal of Antibiotics*, 57(3), 243–246.

Kelso, G. F., Porteous, C. M., Coulter, C. V., Hughes, G., Porteous, W. K., Ledgerwood, E. C., Smith, R. A. J, & Murphy, M. P. (2001). Selective targeting of a redox-active ubiquinone to mitochondria within cells: antioxidant and antiapoptotic properties. *Journal of Biological Chemistry*, 276(7), 4588–4596.

Köning, T., Kapus, A., & Sarkadi, B. (1993). Effects of equisetin on rat liver mitochondria: evidence for inhibition of substrate anion carriers of the inner membrane. *Journal of Bioenergetics and Biomembranes*, 25(5), 537–545.

Li, H., Gilchrist, C. L. M., Lacey, H. J., Crombie, A., Vuong, D., Pitt, J. I., Lacey, E., Chooi, Y. H., & Piggott, A. M. (2019). Discovery and heterologous biosynthesis of the burnettramic acids: rare PKS-NRPS-derived bolaamphiphilic pyrrolizidinediones from an Australian fungus, *Aspergillus burnettii*. *Organic Letters*, 21(5), 1287–1291.

Link, T. A., Haase, U., Brandt, U., & von Jagow, G. (1993). What information do inhibitors provide about the structure of the hydroquinone oxidation site of ubihydroquinone: cytochrome *c* oxidoreductase? *Journal of Bioenergetics and Biomembranes*, 25(3), 221–232.

Mo, X., Li, Q., & Ju, J. (2014). Naturally occurring tetramic acid products: isolation, structure elucidation and biological activity. *RSC Advances*, 4(92), 50566–50593.

Matsuno-Yagi, A. & Hatefi, Y. (1996). Ubiquinol-cytochrome *c* oxidoreductase. The redox reactions of the bis-heme cytochrome *b* in ubiquinone-sufficient and ubiquinone-deficient systems. *Journal of Biological Chemistry*, 271(11), 6164–6171.

Matsuno-Yagi, A. & Hatefi, Y. (1985). Studies on the mechanism of oxidative phosphorylation. *Journal of Biological Chemistry*, 260(27), 14424–14427.

Newman, D. J. & Cragg, G. M. (2020). Natural products as sources of new drugs over the nearly four decades from 01/1981 to 09/2019. *Journal of Natural Products*, 83(3), 770–803.

Ōmura, S., Asami, Y., & Crump, A. (2018). Staurosporine: new lease of life for parent compound of today's novel and highly successful anti-cancer drugs. *The Journal of Antibiotics*, 71(8), 688–701.

Quek, N. C., Matthews, J. H., Bloor, S. J., Jones, D. A., Bircham, P. W., Heathcott, R. W., & Atkinson, P. H. (2013). The novel equisetin-like compound, TA-289, causes aberrant mitochondrial morphology which is independent of the production of reactive oxygen species in *Saccharomyces cerevisiae*. *Molecular BioSystems*, 9(8), 2125–2133.

Suga, T., Asami, Y., Hashimoto, S., Nonaka, K., Iwatsuki, M., Nakashima, T., Sugahara, R., Shiotsuki, T., Yamamoto, T., Shinohara, Y., Ichimaru, N., Murai, M., Miyoshi, H., Ōmura, S., & Shiomi, K. (2015). Ascosteroside C, a new mitochondrial respiration inhibitor discovered by pesticidal screening using recombinant *Saccharomyces cerevisiae*. *The Journal of Antibiotics*, 68(10), 649–652.

Sakai, K., Unten, Y., Iwatsuki, M., Matsuo, H., Fukasawa, W., Hirose, T., Chinen, T., Nonaka, K., Nakashima, T., Sunazuka, T., Usui, T., Murai, M., Miyoshi, H., Asami, Y., Ōmura, S., & Shiomi, K. (2019). Fusaramin, an antimitochondrial compound produced by *Fusarium* sp., discovered using multidrug-sensitive *Saccharomyces cerevisiae*. *The Journal of Antibiotics*, 72(9), 645–652.

Shang, Z., Li, L., Espósito, B. P., Salim, A. A., Khalil, Z. G., Quezada, M., Bernhardt, P. V., & Capon, R. J. (2015). New PKS-NRPS tetramic acids and pyridinone from an Australian marine-derived fungus, *Chaunopycnis* sp. *Organic & Biomolecular Chemistry*, 13(28), 7795–7802.

Trumpower, B. L. (1990). The protonmotive Q cycle. Energy transduction by coupling of proton translocation to electron transfer by the cytochrome bc_1 complex. *Journal of Biological Chemistry*, 265(20), 11409–11412.

Unten, Y., Murai, M., Yamamoto, T., Watanabe, A., Ichimaru, N., Aburaya, S., Aoki, W., Shinohara, Y., & Miyoshi, H. (2019). Pentenediol-

type compounds specifically bind to voltage-dependent anion channel 1 in *Saccharomyces cerevisiae* mitochondria. *Biochemistry*, 58(8), 1141–1154.

Weinberg, S. & Chandel, N. S. (2015). Targeting mitochondria metabolism for cancer therapy. *Nature Chemical Biology*, 11(1), 9–15.

Watanabe, Y., Suga, T., Narusawa, S., Iwatsuki, M., Nonaka, K., Nakashima, T., Shinohara, Y., Shiotsuki, T., Ichimaru, N., Miyoshi, H., Asami, Y., Ōmura, S., & Shiomi, K. (2017). Decatamariic acid, a new mitochondrial respiration inhibitor discovered by pesticidal screening using drug-sensitive *Saccharomyces cerevisiae*. *The Journal of Antibiotics*, 70(4), 395–399.

Xu, W., Cai, X., Jung, M. E., & Tang, Y. (2010). Analysis of intact and dissected fungal polyketide synthase-nonribosomal peptide synthetase in vitro and in *Saccharomyces cerevisiae*. *Journal of American Chemical Society*, 132(39), 13604–13607.

Yabunaka, H., Kenmochi, A., Nakatogawa, Y., Sakamoto, K., & Miyoshi, H. (2002). Hybrid ubiquinone: novel inhibitor of mitochondrial complex I. *Biochimica et Biophysica Acta*, 1556(2-3), 106–112.